

Critical line of an n -component cubic model

Wenan Guo^{1,5*}, Xiaofeng Qian², Henk W. J. Blöte^{3,2} and F. Y. Wu⁴

¹ *Physics Department, Beijing Normal University, Beijing 100875, P. R. China*

² *Instituut Lorentz, Universiteit Leiden, Niels Bohrweg 2,
Postbus 9506, 2300 RA Leiden, The Netherlands*

³ *Faculty of Applied Sciences, Delft University of Technology,
P.O. Box 5046, 2600 GA Delft, The Netherlands*

⁴ *Department of Physics, Northeastern University,
Boston, Massachusetts 02115, USA*

⁵ *The Abdus Salam International Centre for Theoretical Physics, Trieste, Italy*

(Dated: March 23, 2022)

Abstract

We consider a special case of the n -component cubic model on the square lattice, for which an expansion exists in Ising-like graphs. We construct a transfer matrix and perform a finite-size-scaling analysis to determine the critical points for several values of n . Furthermore we determine several universal quantities, including three critical exponents. For $n < 2$, these results agree well with the theoretical predictions for the critical $O(n)$ branch. This model is also a special case of the (N_α, N_β) model of Domany and Riedel. It appears that the self-dual plane of the latter model contains the exactly known critical points of the $n = 1$ and 2 cubic models. For this reason we have checked whether this is also the case for $1 < n < 2$. However, this possibility is excluded by our numerical results.

PACS numbers: 64.60.Ak, 64.60.Fr, 64.60.Kw, 75.10.Hk

* E-mail: waguo@bnu.edu.cn

I. INTRODUCTION

The n -component cubic model can be defined in terms of vector spins that are restricted to lie along one of n Cartesian axes, but are free to assume the positive or negative direction. Only one vector component is nonzero; it is normalized to be ± 1 . The model can be described by the reduced Hamiltonian

$$\mathcal{H}/k_{\text{B}}T = - \sum_{\langle ij \rangle} [K \vec{s}_i \cdot \vec{s}_j + M(\vec{s}_i \cdot \vec{s}_j)^2], \quad (1)$$

where the index i of the cubic spin \vec{s}_i refers to the sites of the square lattice. The sum on $\langle ij \rangle$ stands for all nearest-neighbor pairs. This model obviously combines Potts degrees of freedom (the choice of the Cartesian axis, which is subject to permutation symmetry) with Ising degrees of freedom which specify the sign of the nonzero component. This is more explicit in the following form of the Hamiltonian

$$\mathcal{H}/k_{\text{B}}T = - \sum_{\langle ij \rangle} (K s_i s_j + M) \delta_{\tau_i \tau_j}, \quad (2)$$

where we represent the sign of the nonzero component of \vec{s}_i by $s_i = \pm 1$ and its Cartesian axis number by $\tau_i = 1, 2, \dots, n$. The corresponding bond weight w_{ij} can be rewritten as

$$\begin{aligned} w_{ij} &= \exp[(K s_i s_j + M) \delta_{\tau_i \tau_j}] \\ &= 1 + \delta_{\tau_i \tau_j} \{\exp(K s_i s_j + M) - 1\} \\ &= 1 + \delta_{\tau_i \tau_j} n \{v + x s_i s_j\} \\ &= \sum_{b_{ij}=0}^1 [\delta_{\tau_i \tau_j} n \{v + x s_i s_j\}]^{b_{ij}}. \end{aligned} \quad (3)$$

In the third line we have used the definitions

$$v \equiv \frac{e^M \cosh K - 1}{n} \quad \text{and} \quad x \equiv \frac{e^M \sinh K}{n}, \quad (4)$$

and in the fourth line we have introduced bond variables $b_{ij} = 0$ or 1 , and the summand is subject to the rule $0^0 = 1$. Thus the partition sum assumes the form

$$Z_{\text{cub}} = \sum_{\{s\}, \{\tau\}} \prod_{\langle ij \rangle} \sum_{b_{ij}=0}^1 [\delta_{\tau_i \tau_j} n \{v + x s_i s_j\}]^{b_{ij}}. \quad (5)$$

Application of the Kasteleyn-Fortuin mapping [1] involves execution of the sum on the Potts-like variables $\{\tau\}$. This leads to

$$Z_{\text{cub}} = n^N \sum_{\{s\}} \left[\prod_{\langle ij \rangle} \sum_{b_{ij}=0}^1 \{v + x s_i s_j\}^{b_{ij}} \right] n^{n_l}, \quad (6)$$

where N is the number of sites of the lattice. Note that each bond (by which we mean a bond variable $b_{ij} = 1$) contributes, through the Kronecker δ , also a factor $1/n$, unless it closes a loop. The latter condition is accounted for by the factor n^{n_l} , where n_l is the number of loops formed by the bond variables. Each configuration of bond variables b_{ij} defines a graph on the square lattice covering those and only those edges for which $b_{ij} = 1$. For the special case

$$\cosh K = e^{-M} \quad \text{or} \quad v = 0, \quad (7)$$

the partition sum reduces, after execution of the sum on $\{s\}$, to

$$Z_{\text{cub}} = (2n)^N \sum_{\{b\}} x^{n_b} n^{n_l}, \quad (8)$$

where the sum on $\{b\}$ contains only ‘even’ graphs in which every site is connected to an even number of bonds $b_{ij} = 1$. The odd graphs, while included in the sums on the b_{ij} in Eq. (6), do not survive the sum on $\{s\}$. The number of bonds in the graph $\{b\}$ is denoted $n_b \equiv \sum_{\langle ij \rangle} b_{ij}$.

The cubic loop model described by Eq. (8), is subject to the restriction $|xn| \leq 1$ because of Eq. (7). This model, and the model defined by Eq. (1) with $M = 0$, (both on the square lattice) have already been investigated by a transfer-matrix method [2]. That work included a determination of the temperature exponent. The results for $n < 2$ were in agreement with a conjecture of Cardy and Hamber [3] and the analysis of Nienhuis [4]. However, the latter work applies to the n -component cubic model on the honeycomb lattice, of which the graph expansion reduces to that of the $O(n)$ model. For other lattices, no such direct correspondence exists, and the relevance of the results of Ref. 4 for the cubic model on the square lattice thus needs further justification. This is provided by renormalization arguments that predict that cubic anisotropy is irrelevant [5] for $n < 2$. However, for $n = 2$ it is marginal and indeed the temperature exponent does not agree with the $O(2)$ model [2].

The work of Ref. 2 did not include results for the interval $1 < n < 2$, where the emphasis lies of the present work. Furthermore, the present analysis will purportedly yield more information about universal quantities.

The outline of this paper is as follows. Section II discusses a duality transformation in a three-dimensional parameter space containing the cubic model Eq. (8). This transformation suggests a possible form of the critical line of the cubic model. However, transfer-matrix calculations, defined in Sec. III, yield numerical results listed in Sec. IV, which show that

this form is not applicable. The universal properties of the cubic model are investigated in Sec. V. The paper concludes with a short discussion in Sec. VI.

II. SELF-DUAL PLANE OF THE (N_α, N_β) MODEL

The partition function of the (N_α, N_β) model [6] is defined as

$$Z_{(m,n)}(e^{K_0}, e^{K_1}, e^{K_2}, e^{K_3}) \equiv \sum_{\sigma=1}^m \sum_{\tau=1}^n \prod_{\text{edges}} B(\sigma, \tau | \sigma', \tau'), \quad (9)$$

where $m = N_\alpha$, $n = N_\beta$, and

$$B(\sigma, \tau | \sigma', \tau') \equiv \exp[K_0 \delta_{\sigma\sigma'} \delta_{\tau\tau'} + K_1 (1 - \delta_{\sigma\sigma'}) \delta_{\tau\tau'} + K_2 \delta_{\sigma\sigma'} (1 - \delta_{\tau\tau'}) + K_3 (1 - \delta_{\sigma\sigma'}) (1 - \delta_{\tau\tau'})]. \quad (10)$$

Just as the cubic model, the model can be viewed as having two Potts spins σ and τ on each lattice site, with allowed values $\sigma = 1, 2, \dots, m$ and $\tau = 1, 2, \dots, n$. These spins interact with nearest-neighbor couplings according to the Boltzmann weights (10). Note that these weights are elements of the $(mn) \times (mn)$ matrix

$$\mathbf{B} = e^{K_0} I_m \otimes I_n + e^{K_1} J_m \otimes I_n + e^{K_2} I_m \otimes J_n + e^{K_3} J_m \otimes J_n, \quad (11)$$

where I_n and J_n are $n \times n$ matrices

$$I_n = \begin{pmatrix} 1 & 0 & \cdots & 0 \\ 0 & 1 & \cdots & 0 \\ \vdots & \vdots & \ddots & \vdots \\ 0 & 0 & \cdots & 1 \end{pmatrix}, \quad J_n = \begin{pmatrix} 0 & 1 & \cdots & 1 \\ 1 & 0 & \cdots & 1 \\ \vdots & \vdots & \ddots & \vdots \\ 1 & 1 & \cdots & 0 \end{pmatrix}. \quad (12)$$

We consider a model on a planar lattice with open boundary conditions. The partition sum (9) possesses the duality relation [7]

$$Z_{(m,n)}(e^{K_0}, e^{K_1}, e^{K_2}, e^{K_3}) = (mn)^{1-N_D} Z_{(m,n)}^{(D)}(e^{K_0^*}, e^{K_1^*}, e^{K_2^*}, e^{K_3^*}), \quad (13)$$

where N_D is the number of sites of the dual lattice, and $Z^{(D)}$ the dual partition function, with Boltzmann weights also given by Eq. (10) but with the K_i replaced by the dual weights

K_i^* . The latter weights were shown [7] to be equal to the eigenvalues of the matrix \mathbf{B} . For the (m, n) model, these are [6]

$$\begin{pmatrix} e^{K_0^*} \\ e^{K_1^*} \\ e^{K_2^*} \\ e^{K_3^*} \end{pmatrix} = \begin{pmatrix} 1 & m-1 & n-1 & (m-1)(n-1) \\ 1 & -1 & n-1 & -(n-1) \\ 1 & m-1 & -1 & -(m-1) \\ 1 & -1 & -1 & 1 \end{pmatrix} \begin{pmatrix} e^{K_0} \\ e^{K_1} \\ e^{K_2} \\ e^{K_3} \end{pmatrix}. \quad (14)$$

Note that (14) implies $e^{(K_i^*)^*} = (mn)e^{K_i}$, and hence $(Z^{(D)})^{(D)} = Z$, because the number of lattice edges E satisfies Euler's relation $E = N + N_D - 2$ and each lattice edge contributes a factor mn . Eq. (13) then shows that the powers of mn cancel after a pair of duality transformations.

With the notation

$$x_i \equiv e^{K_i}/e^{K_0}, \quad x_i^* \equiv e^{K_i^*}/e^{K_0^*}, \quad (i = 1, 2, 3) \quad (15)$$

the Boltzmann factor can be written as

$$B(\sigma, \tau | \sigma', \tau') = e^{K_0} x_1^{(1-\delta_{\sigma\sigma'})\delta_{\tau\tau'}} x_2^{\delta_{\sigma\sigma'}(1-\delta_{\tau\tau'})} x_3^{(1-\delta_{\sigma\sigma'})(1-\delta_{\tau\tau'})}. \quad (16)$$

Phase transitions will naturally occur in the $\mathbf{x} = (x_1, x_2, x_3)$ parameter space. Thus, the free energy of the (m, n) model is expected to be nonanalytic on a corresponding surface Σ . Generally, as the temperature variable in a given model varies, the point (x_1, x_2, x_3) traces out a certain "thermodynamic" path Γ in \mathbf{x} , and the model exhibits a transition whenever Γ crosses Σ .

Using (14) we find the transformation

$$\begin{aligned} x_1^* &= \frac{1}{\Delta} [1 - x_1 + (n-1)x_2 - (n-1)x_3] \\ x_2^* &= \frac{1}{\Delta} [1 - (m-1)x_1 - x_2 - (m-1)x_3] \\ x_3^* &= \frac{1}{\Delta} [1 - x_1 - x_2 + x_3] \end{aligned} \quad (17)$$

where

$$\Delta = 1 + (m-1)x_1 + (n-1)x_2 + (m-1)(n-1)x_3. \quad (18)$$

The square lattice maps onto itself under the dual transformation, so that the free energies at two points x_i and x_i^* satisfying Eq. (17) are related. One also verifies that the subspace

$$\Delta = \sqrt{mn} \quad (19)$$

is self-dual under the transformation Eq. (17) (but a point in this plane does, in general, not map on itself).

We note that the partition sum of the cubic loop model described by Eq. (5) with $v = 0$, i.e., the model of Eq. (8), can be written as

$$Z_{\text{cub}} = \sum_{\{s\}, \{\tau\}} \prod_{\langle ij \rangle} [1 + n x s_i s_j \delta_{\tau_i \tau_j}]. \quad (20)$$

By introducing $\sigma_k \equiv (s_k + 3)/2$, and the identities

$$s_i s_j = 2\delta_{\sigma_i \sigma_j} - 1 \quad (21)$$

we find the equivalence

$$Z_{\text{cub}} = Z_{(2,n)}(e^{K_0}, e^{K_1}, e^{K_2}, e^{K_3}) \quad (22)$$

with

$$e^{K_0} = 1 + nx, \quad e^{K_1} = 1 - nx, \quad e^{K_2} = e^{K_3} = 1 \quad (23)$$

or

$$x_1 = \frac{1 - nx}{1 + nx}, \quad x_2 = \frac{1}{1 + nx}, \quad x_3 = \frac{1}{1 + nx}. \quad (24)$$

This specifies the mapping of the n -component cubic loop model on the $(N_\alpha = 2, N_\beta = n)$ model. Using the dual transformation (17), this gives rise to

$$x_1^* = x_3^* = x, \quad x_2^* = 0. \quad (25)$$

Hence the dual thermodynamic path Γ of the cubic loop model is the straight line connecting $(0, 0, 0)$ and $(1, 0, 1)$, a result valid for all n .

For two special cases, namely $n = 1$ and $n = 2$, the critical point of the cubic loop model sits at the intersection of the critical surface Σ and the thermodynamic path Γ in the $x_2 = 0$ plane.

We first consider the case $n = 1$, or $\delta_{\tau_i \tau_j} = 1$, in which the model simply reduces to the Ising model. The Boltzmann factor (16) assumes the form

$$B(\sigma, \tau | \sigma', \tau') = e^{K_0} x_1^{1 - \delta_{\sigma \sigma'}} \quad (26)$$

for any values of x_2, x_3 . The critical surface is thus $x_1 = \sqrt{2} - 1$. This plane intersects the thermodynamic path Γ at $x_1 = x_3 = x = \sqrt{2} - 1$, so that the critical point of the cubic loop model is $x_c = \sqrt{2} - 1$.

For the case $n = 2$, the model, i.e., the $(2, 2)$ model, is the well-known Ashkin-Teller model [8]. The shape and location of Σ have been discussed by Wu and Lin [9]. The thermodynamic path Γ crosses the critical surface Σ at $x_1 = x_3 = 1/2$ within the $x_2 = 0$ plane [9]. Thus the critical point of the cubic loop model occurs at $x_c = 1/2$.

While it is known that most of the self-dual plane of the (N_α, N_β) model is noncritical, it is interesting that for both $n = 1$ and $n = 2$, the critical points of the cubic loop model are actually located in the self-dual plane. If this is true for general $1 < n < 2$, we would have

$$1 + x_1 + (n - 1)x_3 = \sqrt{2n} \quad (27)$$

on the $x_2 = 0$ plane, and $x_1 = x_3 = x$, because the critical point lies on the thermodynamic path Γ . Thus the critical value of x would be

$$x_c(n) = (\sqrt{2n} - 1)/n \quad \text{for } 1 \leq n \leq 2. \quad (28)$$

This possibility will be investigated numerically in Sec. IV.

III. THE TRANSFER MATRIX

The transfer-matrix method used here is related to that used in Ref. 2, and it uses in addition some of the techniques described in Refs. 10 and 11 for the random-cluster and the $O(n)$ model respectively. The full description of the transfer matrix is somewhat elaborate, and here we only provide a general outline, supplemented with more detailed information where the procedure is different from those in the references given.

As in Ref. 2, the transfer matrix is constructed on the basis of a graph representation of the cubic model that allows n to be non-integer. However, the present work is restricted to the case $v = 0$, so that the graphs are restricted to be even. This allows the use, given a system size, of a smaller transfer matrix than that used in Ref. 2. We define the model on an $L \times m$ lattice \mathcal{L}_m wrapped on a cylinder, such that the finite-size parameter L is the circumference of the cylinder. The definition of the transfer matrix can be illustrated by appending row $m + 1$ and determining how this affects the partition sum of the model. The

lattice \mathcal{L}_m has an open end at row m ; there are L ‘dangling’ edges that will serve to connect to row $m + 1$ later. Whereas the partition sum Eq. (6) allows only for closed loops, the bond configuration on \mathcal{L}_m may be considered a part of a larger graph so that we allow the dangling edges to be occupied by loop segments. But all sites are still restricted to connect to an even number of bonds. For the construction of the transfer matrix, we need a coding of all possible ways (called connectivities) that the dangling bonds can be connected by the graph $\{b\}$ on \mathcal{L}_m . This coding assigns a unique integer $1, 2, \dots$, which will serve as the transfer-matrix index, to each connectivity. Some of the dangling edges may be empty, i.e., $b_{ij} = 0$. The remaining dangling edges, i.e., the dangling bonds, form a ‘dense connectivity’ without vacant positions. Note that these dense connectivities satisfy a ‘well-nestedness’ principle which asserts that, if positions i and k are connected, and j and l are connected, with $i < j < k < l$, then all i, j, k, l must be connected. Thus, these dense connectivities form a subset of the ‘random cluster’ or ‘Whitney’ connectivities defined in Ref. 10. The number of dangling bonds that are connected by a path of bonds must always be even for the cubic model; this restriction does not apply to those of Ref. 10. By simply excluding the odd connectivities, we thus find coding and decoding algorithms for the dense cubic connectivities. The coding of the general cubic connectivities including vacant positions then follows analogous to the case of the ‘magnetic’ connectivities in Ref. 10.

This coding allows one to divide the partition sum $Z^{(m)}$ of the m -row system in contributions corresponding with different connectivities:

$$Z^{(m)} = \sum_{\alpha} Z_{\alpha}^{(m)}. \quad (29)$$

Next, we append a new row l_{m+1} to the lattice: $\mathcal{L}_{m+1} \equiv \mathcal{L}_m \cup l_{m+1}$, and express the restricted partition sums $Z_{\alpha}^{(m+1)}$ as a linear combination of the $Z_{\beta}^{(m)}$. This is possible because the weight due to the newly appended row is completely determined by the bond variables connecting to the appended vertices and the ‘old’ connectivity β , and this information also determines the ‘new’ connectivity α . We use b_{m+1} to denote the $2L$ appended bond variables, and $\mu(\beta, b_{m+1})$ to denote the function that determines α . The weight factor associated with the new row satisfies

$$w(\beta, b_{m+1}) = (2n)^L x^{\Delta n_b} n^{\Delta n_l}, \quad (30)$$

where Δn_b is the number of appended bonds and Δn_l is the number of loops closed by these

bonds. The recursion connecting the restricted sums is

$$Z_{\alpha}^{(M+1)} = \sum_{\beta} T_{\alpha\beta} Z_{\beta}^{(M)}, \quad (31)$$

in which the transfer matrix $T_{\alpha\beta}$ is defined by

$$T_{\alpha\beta} = (2n)^L \sum_{b_{m+1}} \delta_{\alpha, \mu(\beta, b_{m+1})} x^{\Delta n_b} n^{\Delta n_l}. \quad (32)$$

In actual calculations, the transfer matrix is represented as the product of L sparse matrices, each of which appends one new vertex of the $(m+1)$ -th row. The first vertex of a new row increases the number of dangling edges to $L+2$, so that the sparse matrices assume a larger size than $T_{\alpha\beta}$. After appending the last vertex of that row, the number of dangling edges decreases to L . This technical point was described in some detail for the related case of the $O(n)$ model on the square lattice [11].

The sparse-matrix technique makes it unnecessary to store the full transfer matrix \mathbf{T} . Some of its eigenvalues can be obtained by repeated multiplication of a vector by \mathbf{T} , and analysis of the resulting vector sequence. Since $T_{\alpha\beta}$ is not symmetric in general, we used the method of projection to a Hessenberg matrix as described in Ref. 10. We restricted the calculations to vectors with ‘translation symmetry’, i.e., vectors that are invariant under a permutation of connectivities corresponding with a cyclic permutation of the dangling edges. In general, the largest eigenvalue $\Lambda_L^{(0)}$ determines the free energy $f(L)$ per site in the limit of an infinitely long cylinder ($m \rightarrow \infty$):

$$f(L) = L^{-1} \ln \Lambda_L^{(0)}. \quad (33)$$

Furthermore, the next largest eigenvalues $\Lambda_L^{(i)}$ ($i = 1, 2, \dots$) determine the correlation lengths $\xi_i(L)$ of various types of correlation functions. The latter types depend on the symmetry of the corresponding eigenvector and on possible modifications of \mathbf{T} . In particular, the correlation length $\xi_t(L)$ of the energy-energy correlation function is determined by the gap between the two largest eigenvalues:

$$\xi_t^{-1}(L) = \ln(\Lambda_L^{(0)} / \Lambda_L^{(1)}). \quad (34)$$

For the cubic model, magnetic correlations can be represented, in analogy with the $O(n)$ model, by graphs with odd vertices on the correlated sites. For the present model that means sites connected to one or three bonds. The two correlated sites, which are placed far

apart in the length direction of the cylinder, must be connected by the graph, i.e., belong to the same component of the graph. This additional component does not follow the rules of ‘evenness’ listed earlier. The number of dangling bonds at the open end of the cylinder (between the correlated sites) connecting to the additional odd vertex must be odd. To describe such ‘magnetic’ graphs we define a new set of connectivities in which one group of connected dangling bonds is odd. This leads to a modified transfer matrix, which may alternatively be interpreted as the magnetic sector of a larger transfer matrix whose vector space includes both even and odd connectivities. The gap between $\Lambda_L^{(0)}$ and the largest eigenvalue $\Lambda_L^{(2)}$ in the magnetic sector determines the magnetic correlation length $\xi_h(L)$ as

$$\xi_h^{-1}(L) = \ln(\Lambda_L^{(0)}/\Lambda_L^{(2)}) . \quad (35)$$

A different type of magnetic gap is associated with the density of the loops spanning the circumference of the cylinder. The weight of these loops is modified by assigning a bond weight $-x$ to one bond in each row. A loop spanning the circumference contains an odd number of these modified bonds, and its weight thus changes sign. All other loops contain an even number of modified bonds and their weights are thus unchanged. We denote the largest eigenvalue of the modified transfer matrix by $\Lambda_L^{(3)}$. It determines the length scale $\xi_m(L)$ that may be associated with the effect of an ‘antiferromagnetic seam’ running along the cylinder. For the critical Ising case $n = 1$, both magnetic length scales are related by duality, but this is not so for general n . The corresponding length scale is given by

$$\xi_m^{-1}(L) = \ln(\Lambda_L^{(0)}/\Lambda_L^{(3)}) . \quad (36)$$

In the actual transfer-matrix calculations, we have used finite sizes up to $L = 15$ in the nonmagnetic sector, which then has dimensionality 2 004 032, and up to $L = 14$ in the magnetic sector, which then has dimensionality 3 856 582.

IV. DETERMINATION OF THE CRITICAL LINE OF THE CUBIC MODEL

The asymptotic behavior of the magnetic correlation length $\xi_h(L)$ near a critical point can be expressed in terms of the scaled gap

$$X_h(t, u, L) \equiv \frac{L}{2\pi\xi_h(t, u, L)} , \quad (37)$$

where t parametrizes the distance to the critical point, and u represents an irrelevant field. Renormalization arguments [12], scaling [13], and conformal invariance [14] predict that for large L

$$X_h(t, u, L) \simeq X_h + a_1 L^{y_t} t + b_1 L^{y_u} u + \dots, \quad (38)$$

where X_h is the magnetic scaling dimension, y_t the temperature exponent, and y_u the exponent of the field u , and a_1 and b_1 are unknown amplitudes. Further corrections may also be present. Since we have an algorithm available that calculates $X_h(t, u, L)$ (with t and u expressed as a function of x), we can estimate the critical point by numerically solving x in the equation

$$X_h(x, L) = X_h(x, L + 1), \quad (39)$$

which is a form of ‘phenomenological renormalization’ [15]. After substitution of Eq. (38) one finds that, at the solution, t and u satisfy

$$t \propto u L^{y_u - y_t}. \quad (40)$$

Since $y_t > 0$ and $y_u < 0$, we expect that $t \rightarrow 0$ for $L \rightarrow \infty$, i.e., the solutions of Eq. (39), which we denote $x^{(0)}(L)$, converge to the critical point. These solutions were fitted by solving for $x^{(1)}(L)$, $c^{(1)}(L)$ and $y_u - y_t$ in the three following equations with $L' = L, L - 1$, and $L - 2$:

$$x^{(0)}(L') = x^{(1)}(L) + c^{(1)}(L) L'^{y_u - y_t}, \quad (41)$$

which leads to a sequence $x^{(1)}(L)$ that is shorter than the original sequence $x^{(0)}(L)$ but usually shows faster apparent convergence. Another iteration step can be attempted on the basis of

$$x^{(1)}(L') = x^{(2)}(L) + c^{(2)}(L) L'^{y_u' - y_t}, \quad (42)$$

which may lead to even better estimates of the critical point.

A similar analysis of the critical point can be performed on the basis of the scaled interface gap

$$X_m(t, u, L) \equiv \frac{L}{2\pi\xi_m(t, u, L)}, \quad (43)$$

using the same type of fits as for the scaled magnetic gap.

We have also attempted to find solutions of Eq. (39) with ξ_h replaced by the energy-energy correlation length, but here complications arise. The functions $X_t(x, L)$ typically display an extremum near the critical point, and solutions of the scaling equation Eq. (39),

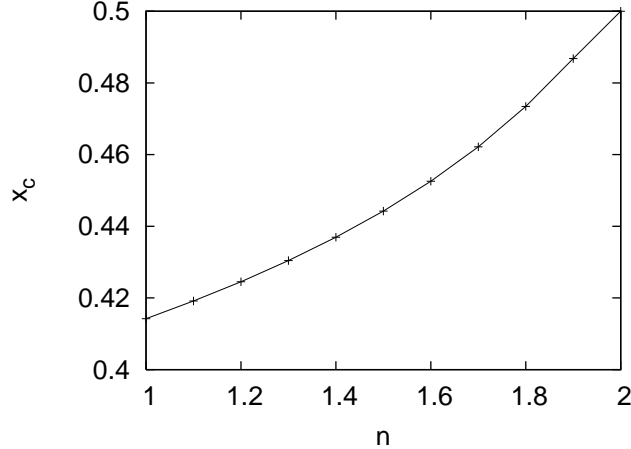


FIG. 1: Critical points of the $v = 0$ cubic model. The data points show the numerical results of the transfer-matrix analysis, and the curve is added as a guide to the eye. The estimated error bars are smaller than the size of the symbols.

with X_t instead of X_h , do not always exist. In particular for $n > 1$ we did not obtain a satisfactory set of solutions, and we have not pursued this way to obtain further data for the critical point. Instead, we located the extremum of $X_t(x, L)$ as a function of x . The finite-size-scaling equation for the correlation length indicates that this extremum will converge to the critical point.

The estimated critical points are shown in Fig. 1. For $1 < n < 2$ they do not agree with Eq. (28). For instance, that equation would predict $x_c = 0.48803 \dots$ for $n = 1.5$, which is incompatible with the numerical result (see also Table I). Thus we have to conclude that Eq. (28), which does indeed lack a solid basis, is not valid for all values of n .

Several modified fitting procedures were applied. Assuming that the cubic model reduces to the $O(n)$ universality class, we have analytic evidence for the values of y_u and y'_u as a function of n . First, according to the renormalization scenario, the cubic perturbation of the $O(n)$ symmetry corresponds with an irrelevant field with an exponent [5]

$$y_c = \frac{(1-g)(1+3g)}{2g}, \quad (44)$$

where $\cos(\pi g) = -n/2$ and $1 \leq g \leq 2$. Corrections due to this field are expected to be serious for $n \rightarrow 2$, since $y_c \rightarrow 0$. Second, irrelevant temperature-like fields may correspond with some scalar operators whose dimensions are entries $X_{1,q}$ with $q > 3$ in the Kac table

TABLE I: Critical points x_c as determined from the scaling formulas for the magnetic and interface correlation length for system sizes L and $L + 1$, and from the extrema of the energy-like correlation length as x is varied. The estimated numerical uncertainty in the last decimal place is shown in parentheses. The ‘best estimates’ are based on the results in the two preceding columns and on an analysis of the minima in the functions $X_t(x, L)$ as described in the text. For $n = 1$ we find accurate agreement with the exact result $x_c = \sqrt{2} - 1$, and for $n = 2$ with $x_c = 1/2$.

n	x_c (from X_h)	x_c (from X_m)	x_c (best estimates)
1.0	0.4142134 (2)	0.4142135 (1)	0.4142135 (1)
1.1	0.419155 (5)	0.419154 (2)	0.419154 (2)
1.2	0.424530 (5)	0.424527 (2)	0.424528 (2)
1.3	0.43042 (1)	0.430415 (5)	0.430416 (5)
1.4	0.43695 (2)	0.436935 (5)	0.43694 (1)
1.5	0.44423 (5)	0.44424 (1)	0.44424 (1)
1.6	0.45257 (5)	0.45254 (1)	0.45254 (1)
1.7	0.46212 (5)	0.46214 (1)	0.46214 (1)
1.8	0.4736 (1)	0.47345 (2)	0.47346 (2)
1.9	0.4869 (2)	0.48673 (5)	0.48675 (5)
2.0	0.5000000 (1)	0.4999999 (1)	0.5000000 (1)

[16, 17]

$$X_{p,q} = \frac{[p(m+1) - qm]^2 - 1}{2m(m+1)} \quad (45)$$

with $m = 1/(g - 1)$ for the cubic model [18]. For $q = 5$ we find an irrelevant exponent

$$y_i = \frac{6g - 12}{g}. \quad (46)$$

which has small values for $n > 0$ but becomes marginal when $n \rightarrow -2$. The final results, and their estimated errors, were obtained from the analyses of the three types of scaled gap, and the degree of consistency between different types of fits mentioned above. The best estimates obtained from $X_h(t, u, L)$ and $X_m(t, u, L)$, and the overall best estimates which also include data from $X_t(t, u, L)$, are shown in Table I.

V. UNIVERSAL PROPERTIES OF THE CUBIC MODEL

The asymptotic finite-size dependence of the free energy per site at the critical point is [18, 19]

$$f(L) \simeq f(\infty) + \frac{\pi c}{6L^2}, \quad (47)$$

where c is the conformal anomaly of the model, which characterizes universality classes and determines sets of critical exponents [20, 21]. We have calculated the finite size data for the free energy at the extrapolated critical points, and estimated c as $c^{(1)}(L)$ from the free energy density for two consecutive system sizes by solving

$$c^{(1)}(L) = 6[f(L) - f(L+1)]/[\pi\{1/L^2 - 1/(L+1)^2\}]. \quad (48)$$

This leads to a sequence of estimates of c that can be extrapolated by means of power-law fits, analogous to the procedure used to determine the critical points. After a second iteration step, the estimates of c seem almost converged, in the sense that the results for the largest few values of L display differences of only a few times 10^{-5} . But at the same time these data display a shallow extremum (except for $n = 1$ and 2 , where the apparent convergence is much better), so that it is difficult to estimate the uncertainty in the extrapolated results. Because the first iteration step shows that the finite-size dependence of the estimates of c is close to -2 , we have also applied iteration steps with the exponent fixed at this value. The results were similar to those obtained with free exponents, and again displayed a shallow extremum. Under these circumstances we made a crude error estimate of ten times the difference between the two estimates for the largest available L values, after two iteration steps. The best estimate was taken by extrapolating the last two estimates, using again ten times the aforementioned difference. A better apparent convergence was found when a fixed exponent $y_c - 2$ was used in the second iteration step. The results are shown in Table II. The numerical errors were estimated from the finite-size dependence of the results of the last fit procedure, except for $n = 1.9$, where the error bars of both fit procedures did not overlap and we used the difference between both types of fit instead. Most of our results are in good agreement with the theoretical values:

$$c = 1 - \frac{6(g-1)^2}{g}. \quad (49)$$

which follow after the substitution of the formula [18] $m = 1/(g-1)$ in the relation [20] between m and c , i.e., $c = 1 - 6/[m(m+1)]$. But the result for $n = 1.9$ does not agree well

TABLE II: Conformal anomaly and temperature scaling dimension X_t as determined by transfer-matrix calculations described in the text. Estimated error margins in the last decimal place are given in parentheses. For comparison, we include the theoretical values of the $O(n)$ model for $n < 2$, and of the Ashkin-Teller model for $n = 2$. The numerical results are indicated by ‘num’, theoretical values by ‘theory’.

n	$c(\text{num})$	$c(\text{theory})$	$X_t(\text{num})$	$X_t(\text{theory})$
1.0	0.50000 (1)	0.50000	1.000000 (1)	1.00000
1.1	0.54820 (2)	0.54820	1.0428 (5)	1.04269
1.2	0.59640 (2)	0.59639	1.0890 (5)	1.08840
1.3	0.64465 (5)	0.64465	1.1385 (5)	1.13782
1.4	0.6931 (1)	0.69309	1.192 (1)	1.19187
1.5	0.7418 (1)	0.74184	1.251 (2)	1.25189
1.6	0.7912 (1)	0.79106	1.319 (2)	1.31996
1.7	0.8410 (1)	0.84096	1.405 (5)	1.39962
1.8	0.8920 (2)	0.89186	1.49 (2)	1.49783
1.9	0.9464 (9)	0.94432	1.60 (5)	1.63279
2.0	1.00000 (1)	1	1.500000 (1)	3/2

with the theoretical value; we note that the small value of the cubic crossover exponent, which becomes marginal at $n = 2$, may well lead to imprecise results and error estimates.

Next, we analyze the results for the magnetic gaps. After substitution of the solutions of Eq. (39), which behave as Eq. (40), in Eq. (38), one finds that the magnetic scaled gaps at the solutions converge to X_h as:

$$X_h(L) = X_h + ruL^{y_u} + \dots, \quad (50)$$

where r is an unknown constant. The magnetic scaled gaps at the solutions of the scaling equation in the previous section were already available. They were fitted using a similar procedure as used for the determination of the critical points. We found that the leading irrelevant exponent was consistent with the predicted cubic perturbation exponent given in Eq. (44), and we accordingly treated y_u as a known parameter in the fits. The extrapolated

TABLE III: The magnetic dimension X_h and the interface dimension X_m as extrapolated from their values at the solutions of the scaling equation of the correlation length. Estimated numerical uncertainty in the last decimal place are given in parentheses. For comparison, we include the theoretical values of the $O(n)$ model for $n < 2$, and of the Ashkin-Teller model for $n = 2$. The numerical results are indicated by '(num)', the theoretical values by '(theory)'.

n	$X_h(\text{num})$	$X_h(\text{theory})$	$X_m(\text{num})$	$X_m(\text{theory})$
1.0	0.12499 (1)	0.12500	0.12499 (1)	1/8
1.1	0.12647 (1)	0.12668	0.14105 (5)	0.14101
1.2	0.1280 (1)	0.12826	0.15814 (5)	0.15815
1.3	0.1296 (1)	0.12973	0.1767 (1)	0.17668
1.4	0.1307 (1)	0.13107	0.1969 (2)	0.19695
1.5	0.1316 (1)	0.13224	0.2195 (5)	0.21946
1.6	0.1320 (1)	0.13319	0.244 (1)	0.24499
1.7	0.1335 (3)	0.13382	0.274 (2)	0.27486
1.8	0.1308 (2)	0.13393	0.313 (2)	0.31169
1.9	0.128 (1)	0.13300	0.350 (5)	0.36230
2.0	0.12498 (1)	1/8	0.37500 (1)	3/8

magnetic scaling dimensions are shown in Table III. Again, different fit procedures, with the finite-size exponent left free, and more iteration steps, were applied. The error estimates are based on the apparent convergence and on the differences between the various types of fit. The final results appear to agree with the theoretical values for the $O(n)$ universality class [4]:

$$X_h = \frac{g}{8} - \frac{(1-g)^2}{2g}. \quad (51)$$

where we note that the Ashkin-Teller model (or $(2, 2)$ model) has the same magnetic scaling dimension [22, 23] $X_h = 1/8$ as the $O(2)$ model.

A similar analysis was performed on the scaled interface gaps at the solutions of the scaling equation for interface scaled gap. These gaps converge to the interface scaling dimension. The results for the interface scaling dimension are shown in Table III. These results are to be compared with the known interface exponent in the $O(n)$ universality class [11], which

are given by the entry $p = 1, q = 2$ in the Kac table:

$$X_m = \frac{3}{2g} - 1. \quad (52)$$

which is obtained by the substitution of $m = 1/(g - 1)$ in the more common form $X_{1,2} = [(m - 1)^2 - 1]/2m(m + 1)$ of the Kac formula.

Our result for X_m at $n = 2$ is different from $X_{1,2} = 1/2$ and thus illustrates that the $n = 2$ cubic loop model falls outside the $O(2)$ universality class. It is to be compared with results for the Ashkin-Teller model [23, 24] which are also summarized by Baxter [25]. In the notation used there, we have the exact result $\beta_e^{8V} = 3/4$ for the end point of the Ashkin-Teller line at $K \rightarrow \infty$. This exponent may, in our notation, be put equal to $X_m/(2 - X_t)$ where $X_t = 3/2$. This does indeed lead to $X_m = 3/8$.

We also calculated the temperature scaled gaps $X_t(x, L)$ at the extrapolated critical points. We expect the following behavior of these gaps:

$$X_t(L) = X_t + puL^{y_u} + \dots, \quad (53)$$

where p is another unknown constant. Similar fits as before lead to results for the temperature scaling dimension that are included in Table II. The results agree with the theoretical prediction [4] for the $O(n)$ model

$$X_t = \frac{4}{g} - 2, \quad (54)$$

except for the case $n = 2$, where our numerical result goes to $3/2$ in accordance with the exact result [23, 24] for the temperature scaling dimension of the Ashkin-Teller model for $K \rightarrow \infty$.

VI. DISCUSSION

In general, the discreteness of the n -component cubic model defined by Eq. (1) will enforce the existence of a long-range ordered phase at sufficiently low temperatures, also for $n > 2$. However, our transfer-matrix calculations for $v = 0$ in Eq. (7) did not yield any evidence for a phase transition to the ordered phase for $n > 2$. The absence of a phase transition is understandable in terms of the parameters K and M in Eq. (1), because Eq. (7) restricts these parameters to $K + M \leq \ln 2$. This quantity, which specifies the energy difference between parallel ($\vec{s}_i \cdot \vec{s}_j = 1$) spins and perpendicular ($\vec{s}_i \cdot \vec{s}_j = 0$) spins, is not sufficient to

reach a long-range-ordered phase for $n > 2$. The maximum value $K + M = \ln 2$ along the critical line is reached for $n = 2$ where $K = \infty$.

For $n \leq 2$ we find clear evidence for a phase transition to the ordered phase. In the interval $1 \leq n \leq 2$ we have determined the critical points of the n -component cubic model as given by Eqs. (1) and (7), or by Eq. (8). For the exactly solved cases $n = 1$ and $n = 2$ we find good agreement with the exact values as given in Table I. Our results for the scaling dimensions, i.e., X_t associated with the temperature, X_h associated with the magnetic field, and X_m associated with the introduction of an antiferromagnetic ‘seam’ in the model, agree accurately with the $O(n)$ universality classes, with the exception of the case $n = 2$ where the model reduces to a special case of the Ashkin-Teller model. For the latter case $n = 2$, our results for the scaling dimensions agree with the exact results for the Ashkin-Teller model. The fact that these scaling dimensions are different from those for the $O(2)$ universality class is related with the cubic anisotropy which may be seen as a perturbation of the $O(n)$ symmetry. This perturbation is irrelevant for $n < 2$ but marginal [5] for $n = 2$. This proof of irrelevance for $n < 2$ applies to small cubic perturbations of the isotropy. Our numerical results show that the cubic perturbation remains irrelevant even in the extreme anisotropic case described by Eqs. (1) and (7). However, when n approaches 2, the exponent y_c associated with the cubic anisotropy field approaches marginality and our numerical results thus become less accurate. The cubic anisotropy is truly marginal at $n = 2$ and parametrizes the Ashkin-Teller model. For this reason, the cubic crossover phenomena are absent for $n = 2$ and the numerical results are again relatively accurate. The temperature scaling dimension of the cubic model and its consistency with $O(n)$ universality were already determined [2] for a range $n \leq 1$. The present results extend the range of n and provide additional evidence concerning the dimensions X_h and X_m . The numerical accuracy of our analysis is such that the $O(n)$ universality of the cubic model seems reasonably convincing. We note that numerical results for the $O(n)$ model on the square lattice [11] are even more accurate; however, for that case the exact critical point is known, and the cubic anisotropy field, and thereby the leading corrections to scaling, vanish.

Acknowledgments

This research is supported in part by the Dutch FOM foundation (‘Stichting voor Fundamenteel Onderzoek der Materie’) which is financially supported by the NWO (‘Nederlandse Organisatie voor Wetenschappelijk Onderzoek’), by the National Science Foundation of China under Grant #10105001, and by a grant from Beijing Normal University.

- [1] P. W. Kasteleyn and C. M. Fortuin, J. Phys. Soc. Jpn. (suppl.) **46**, 11 (1969).
- [2] H. W. J. Blöte and M. P. Nightingale, Physica A **129**, 1 (1984).
- [3] J. L. Cardy and H. W. Hamber, Phys. Rev. Lett. **45**, 499 (1980).
- [4] B. Nienhuis, Phys. Rev. Lett. **49**, 1062 (1982); J. Stat. Phys. **34**, 731 (1984).
- [5] B. Nienhuis, in *Phase Transitions and Critical Phenomena* ed. C. Domb and J. L. Lebowitz (Academic, London 1987), Vol. **11**.
- [6] E. Domany and E. K. Riedel, Phys. Rev. B **19**, 5817 (1979); Phys. Rev. Lett. **40**, 561 (1978).
- [7] F. Y. Wu and Y. K. Wang, J. Math. Phys **17**, 439 (1976).
- [8] J. Ashkin and E. Teller, Phys. Rev. **64**, 178 (1943).
- [9] F. Y. Wu and K. Y. Lin, J. Phys. C **7**, L181 (1974).
- [10] H. W. J. Blöte and M. P. Nightingale, Physica A **112**, 405 (1982).
- [11] H. W. J. Blöte and B. Nienhuis, J. Phys. A **22**, 1415 (1989).
- [12] M. Suzuki, Progr. Theor. Phys. **58**, 1142 (1977).
- [13] For reviews, see e.g. M. P. Nightingale in *Finite-Size Scaling and Numerical Simulation of Statistical Systems*, ed. V. Privman (World Scientific, Singapore 1990), and M. N. Barber in *Phase Transitions and Critical Phenomena*, Vol. **8**, eds. C. Domb and J. L. Lebowitz (Academic, New York 1983).
- [14] J. L. Cardy, J. Phys. A **17**, L385 (1984).
- [15] M. P. Nightingale, Phys. Lett. A **59**, 486 (1977); Proc. Kon. Ned. Ak. Wet. B **82**, 235 (1979).
- [16] D. Friedan, Z. Qiu and S. Shenker, Phys. Rev. Lett. **52**, 1575 (1984).
- [17] V. G. Kac, in "Group Theoretical Methods in Physics", ed. W. Beiglbock en A. Bohm, Lecture Notes in Physics, Vol. **94**, 441 (Springer, New York, 1979).
- [18] H. W. J. Blöte, J. L. Cardy and M. P. Nightingale, Phys. Rev. Lett. **56**, 742 (1986).

- [19] I. Affleck, Phys. Rev. Lett. **56**, 746 (1986).
- [20] J. L. Cardy, in *Phase Transitions and Critical Phenomena* ed. C. Domb and J. L. Lebowitz (Academic, London 1987), Vol. **11**.
- [21] A. A. Belavin, A. M. Polyakov and A. B. Zamolodchikov, J. Stat. Phys. **34**, 763 (1984).
- [22] I. G. Enting, J. Phys. A **8**, L35 (1975).
- [23] M. P. M. den Nijs, Phys.Rev. B **23**, 6111 (1981).
- [24] H. J. F. Knops, Ann. Phys. (N. Y.) **128**, 448 (1980).
- [25] R. J. Baxter, *Exactly Solved Models in Statistical Mechanics* (Academic, London, 1982).